

USPAS Course on Recirculated and Energy Recovered Linacs

I. V. Bazarov

Cornell University

G. A. Krafft and L. Merminga

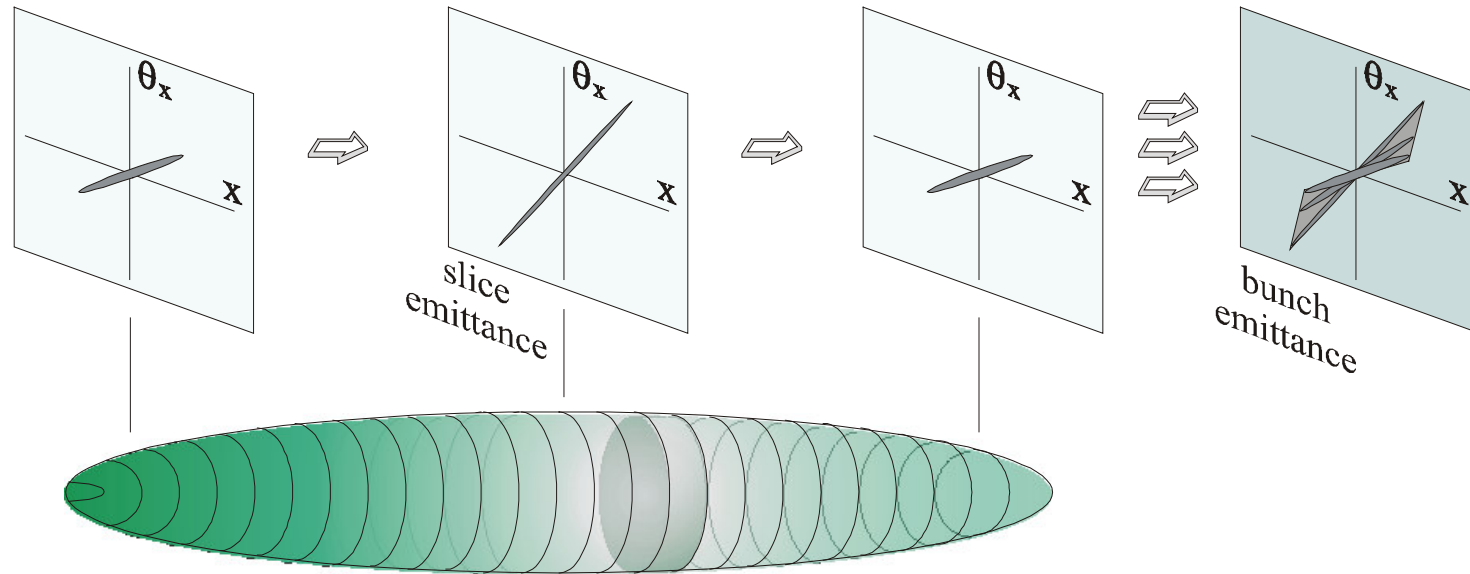
Jefferson Lab

Injector II: Beam Dynamics II and Technology

Contents

- Space charge
- Debye length
- Equilibrium distribution
- Envelope equation
- Emittance compensation
- Computational aspects
- Optimal initial pulse distribution
- Technology of DC/NCRF/SRF guns

Space charge



In a typical bunched beam from a gun, both charge and current density are functions of transverse & longitudinal coordinates. This makes space charge dominated behavior highly nonlinear.

For beam envelope equation we will assume that ρ and J_z are independent of transverse coordinate and that the beam is not bunched (aspect ratio $\ll 1$).

“Collisional” vs. “smooth” self-fields

It would seem that the easiest approach is to calculate Lorentz force of all electrons directly (this would encompass practically *all* the behavior of the beam). This is not feasible because the number of evaluations for each time step is $\sim N^2$, with $N \sim 10^{10}$. Taking the fastest supercomputer with 100 TFLOPS, one estimates \sim year(s) per time step (and one may need something like $\sim 10^4$ steps).

Instead, people use macroparticles in computer simulations with the same e/m ratio

When $N \rightarrow \infty$ forces are smooth; when $N \rightarrow 1$ grainy collisional forces dominate. Envelope equation assumes the first scenario.

How to determine quantitatively “collisional” vs. “smooth” behavior of the space charge in the beam?

Debye length and plasma frequency

Three characteristic lengths in the bunch:

a bunch dimension; l_p interparticle distance; λ_D Debye length

Interactions due to Coulomb forces are long-range; Debye length is a measure of how 'long' (screen-off distance of a local perturbation in charge).

for nonrelativistic case:

$$\omega_p = \sqrt{\frac{e^2 n}{\epsilon_0 m}}, \sigma_{v_x} = \sqrt{\frac{k_B T}{m}}$$

$$\lambda_D = \sqrt{\frac{\epsilon_0 k_B T}{e^2 n}}$$

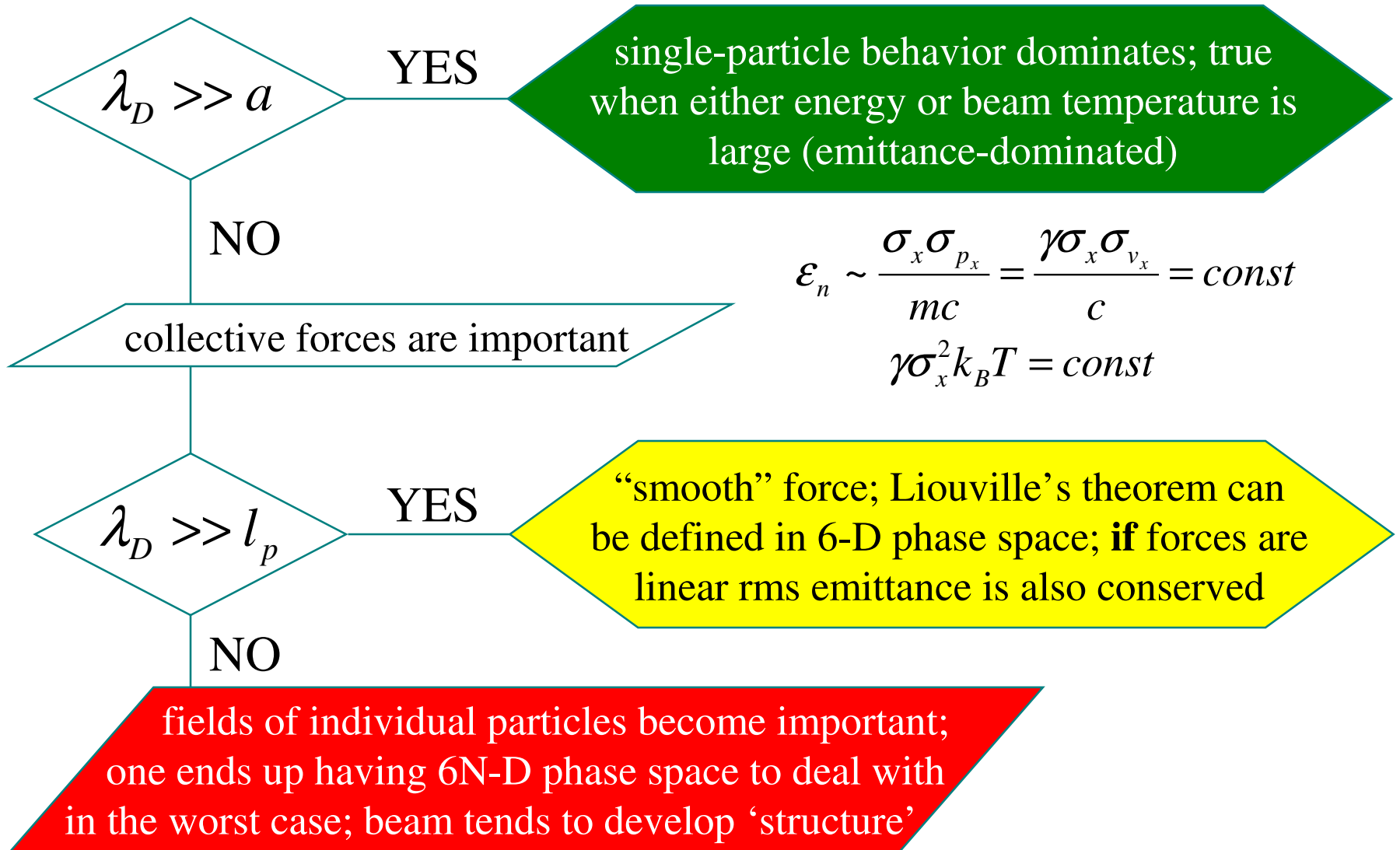
$$\lambda_D \equiv \frac{\sigma_{v_x}}{\omega_p}$$

for relativistic case:

$$\omega_p = \sqrt{\frac{e^2 n}{\epsilon_0 m \gamma^3}}, \sigma_{v_x} = \sqrt{\frac{k_B T}{m \gamma}}$$

$$\lambda_D = \sqrt{\frac{\gamma^2 \epsilon_0 k_B T}{e^2 n}}$$

Debye length: beam dynamics scenarios



$$\mathcal{E}_n \sim \frac{\sigma_x \sigma_{p_x}}{mc} = \frac{\gamma \sigma_x \sigma_{v_x}}{c} = \text{const}$$

$$\gamma \sigma_x^2 k_B T = \text{const}$$

Equilibrium distribution

Similar to thermodynamics and plasma physics, there may exist equilibrium particle distributions (i.e. those that remain stationary). Vlasov theory allows one to find such distributions (assumes collisions are negligible, but they are the ones responsible to drive the distribution to the equilibrium!). Without the derivation, Vlasov-Maxwell equations for equilibrium distributions $f(q_i, p_i, t)$ (i.e. no explicit time dependence, $\partial/\partial t = 0$):

$$\sum_{i=1}^3 \left[\frac{\partial f}{\partial q_i} \dot{q}_i + e(\vec{E} + \vec{v} \times \vec{B})_i \frac{\partial f}{\partial p_i} \right] = 0$$

$$\vec{\nabla} \times \vec{E} = 0$$

$$\vec{\nabla} \cdot \vec{E} = \frac{e}{\epsilon_0} \int f d^3p$$

$$\vec{\nabla} \times \vec{B} = \mu_0 e \int \vec{v} f d^3p$$

$$\vec{\nabla} \cdot \vec{B} = 0$$

Equilibrium distribution (contd.)

In particular, in a focusing channel, equilibrium transverse density obeys a well-known Boltzmann relation

$$n(r) = n(0) \exp\left[-\frac{e\phi(r)}{k_B T_{\perp}}\right]$$

$$\phi(r) = \phi_{ext}(r) + \frac{1}{\gamma^2} \phi_{self}(r)$$

$$e\phi_{ext}(r) = \gamma m \omega_0^2 r^2 / 2$$

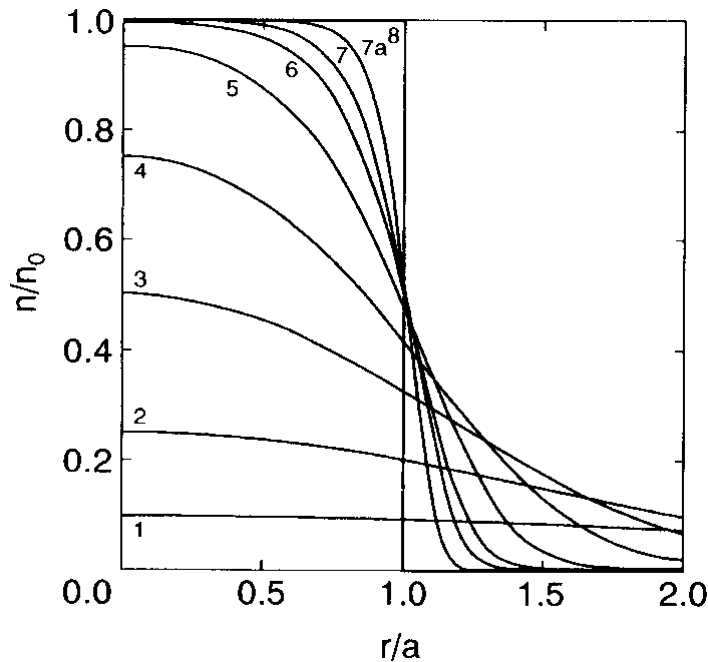
$$\phi_{self}(r) = -\int_0^r \int_0^{\hat{r}} dr d\hat{r} \left(\frac{e}{\epsilon_0 r} \hat{r} n(\hat{r}) \right)$$

Equilibrium distribution (contd.)

Analytically, two extreme cases

$$k_B T \rightarrow 0 \quad (\lambda_D / a \rightarrow 0) \quad n(r) = \begin{cases} n_0 = \text{const}, & \text{for } r \leq a \\ 0, & \text{for } r > a \end{cases} \quad \text{uniform}$$

$$\varphi_{\text{self}} \rightarrow 0 \quad (\lambda_D / a \geq 1) \quad n(r) = n_0 \exp\left[-\frac{\gamma m \omega_0^2 r^2}{2k_B T_{\perp}}\right] \quad \text{Gaussian}$$



Curve	$n(0)/n_0$	$\lambda_D(0)/a_0$	Ka^2/ϵ^2
1	0.1	4.82	0.054
2	0.25	1.81	0.153
3	0.5	0.795	0.396
4	0.75	0.432	0.893
5	0.95	0.229	2.51
6	0.995	0.145	6.00
7	0.9995	0.107	10.9
7a	0.999995	0.0710	24.8
8	1	0	∞

Perveance and characteristic current

Let's derive beam envelope equation (i.e. we assume that self-forces are smooth). We have almost derived the equation already (previous lecture's paraxial ray equation). Two terms are missing – due to space charge and emittance ‘pressure’.

Uniform laminar beam in the absence of external forces:

$$\gamma m \ddot{r} = \frac{e I r}{2 \pi \epsilon_0 a^2 \beta c \gamma^2}, \text{ using } \dot{r} = \beta^2 \gamma^2 r'' \rightarrow r'' = \frac{e I r}{2 \pi \epsilon_0 a^2 m c^3 \beta^3 \gamma^3}$$

$$\ddot{r} = \frac{\omega_p^2}{2} r$$

$$r'' = \frac{K}{a^2} r$$

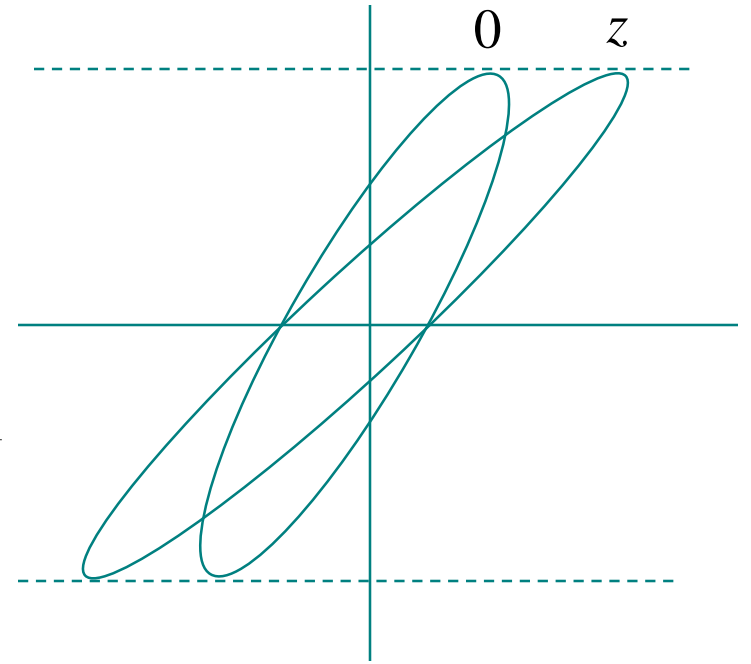
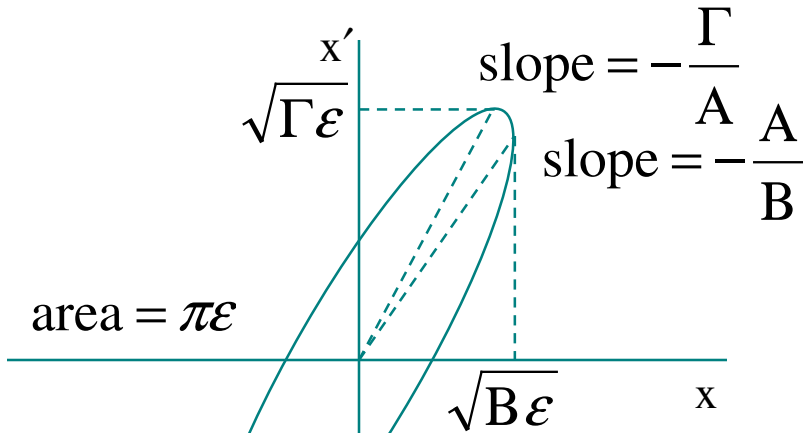
$$r_m r_m'' = K \quad \text{for } r_m = a$$

$$\omega_p^2 = \frac{e I}{\pi \epsilon_0 m c \beta \gamma^3 a^2}$$

$$K = \frac{I}{I_0} \frac{2}{\beta^3 \gamma^3}$$

$$I_0 = \frac{4 \pi \epsilon_0 m c^3}{e} \approx \frac{1}{30} \frac{m c^2}{e} = 17 \text{ kA}$$

Emittance 'pressure' term



$$\Sigma = \langle \vec{x}^T \vec{x} \rangle = \begin{bmatrix} \langle xx \rangle & \langle xx' \rangle \\ \langle x'x \rangle & \langle x'x' \rangle \end{bmatrix} = \epsilon \begin{bmatrix} B & -A \\ -A & \Gamma \end{bmatrix}$$

det[...] = 1

In a drift $0 \rightarrow z$: $x' \rightarrow x' = \text{const}$ and $x \rightarrow x + x'z$ and

$$\begin{aligned} B &\rightarrow B - 2Az + \Gamma z^2 \\ A &\rightarrow A - \Gamma z \\ \Gamma &\rightarrow \Gamma = \text{const} \end{aligned}$$

For σ_x : $\sigma_x' = -\frac{\sqrt{\epsilon}A}{\sqrt{B}}$, $\sigma_x'' = \frac{\sqrt{\epsilon}}{B\sqrt{B}}$ or $\sigma_x'' - \frac{\epsilon^2}{\sigma_x^3} = 0$

Beam envelope equation

From paraxial ray equation with the additional terms, one obtains

$$\sigma'' + \sigma' \frac{\gamma'}{\beta^2 \gamma} + \sigma \frac{1}{\beta^2 \gamma^2} \left[\frac{\gamma'' \gamma}{2} + \left(\frac{eB}{2mc} \right)^2 \right] - \frac{1}{\sigma} \frac{I}{2I_0 \beta^3 \gamma^3} - \frac{1}{\sigma^3} \frac{1}{\beta^2 \gamma^2} \left[\left(\frac{P_\theta}{mc} \right)^2 + \epsilon_n^2 \right] = 0$$

adiabatic

RF focusing
of cavity edge

solenoid

space charge

angular momentum
'increases' emittance

$$\frac{I}{2I_0 \beta \gamma} \gg \frac{\epsilon_n^2}{\sigma^2}, \text{ or } \frac{I}{2I_0 \beta^2 \gamma^2} \gg \frac{\epsilon_n}{B}$$

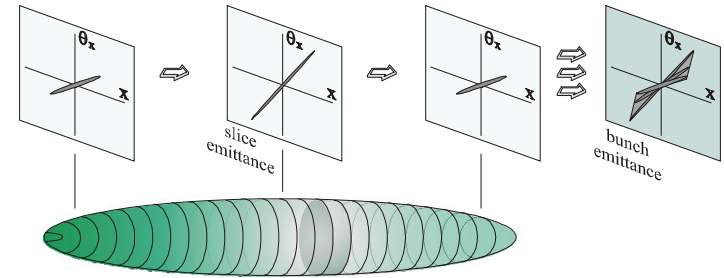
space charge dominated

$$\frac{I}{2I_0 \beta \gamma} \ll \frac{\epsilon_n^2}{\sigma^2}, \text{ or } \frac{I}{2I_0 \beta^2 \gamma^2} \ll \frac{\epsilon_n}{B}$$

emittance dominated

Emittance evolution due to space charge

We have seen that beam will evolve from space-charge dominated to emittance dominated regimes as it is being accelerated. At low energies, various longitudinal ‘slices’ of the bunch experience different forces due to varying current \rightarrow ‘bow-tie’ phase space is common.



Important realization is that much of these space charge emittance growth is reversible through appropriate focusing (and drifts), a so-called emittance compensation. Obviously, this emittance compensation should take place before (or rather as) the beam becomes ultrarelativistic (and emittance-dominated).

Emittance growth in RF guns (without comp.)

Kim analyzed emittance growth due to space charge and RF (NIM A **275** (1989) 201-218). His analysis applies to beam in RF guns. He has found:

$$\epsilon_x^{rf} = \frac{\alpha k_{RF}^3 \sigma_x^2 \sigma_z^2}{\sqrt{2}} \quad \boxed{\alpha \downarrow}$$

$$\alpha = \frac{eE_0}{2mc^2 k_{RF}}$$

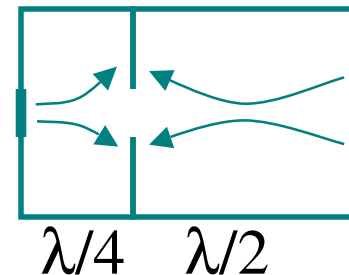
$$\epsilon_x^{sc} = \frac{\pi}{4} \frac{1}{\alpha k_{RF}} \frac{1}{\sin \phi_0} \frac{I_{peak}}{I_0} \mu_x (A) \quad \boxed{\alpha \uparrow}$$

$$\mu_{x,gauss} \approx \frac{1}{3A+5}$$

e.g. 100 MV/m RF gun ($\lambda = 10.5$ cm): $\alpha = 1.64$, phase (to minimize rf emittance) $\phi_0 = 71^\circ$ ($\phi \rightarrow 90^\circ$), laser width and length $\sigma_x = 3.5$ mm, $\sigma_z = 0.6$ mm

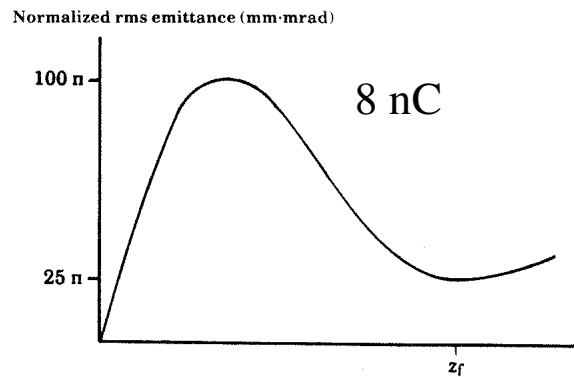
$$\epsilon_x^{rf} = 1.1 \text{ mm - mrad}$$

$$\epsilon_x^{sc} = 4.0 \text{ mm - mrad (1.3 mm - mrad for uniform)}$$



Compensation

Carlsten discovered in simulations that emittance can be brought down and gave a simple explanation for the effect (NIM A **285** (1989) 313-319).



5. Conclusion

A photoelectric injector design analysis has been presented. The emittance growth from the dominant mechanism has been shown to be eliminated with a simple lens configuration, leaving only a small residual emittance resulting from the other mechanisms.

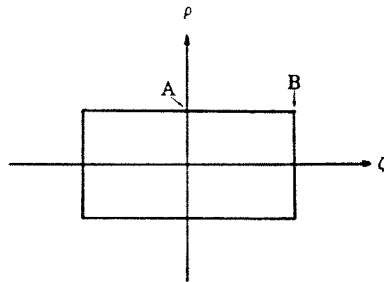


Fig. 2. Typical transverse emittance versus beamline position plot for a photoelectric injector, showing quick initial growth and subsequent reduction for a slug beam and physical description of a slug beam, with internal coordinates ρ and ζ .

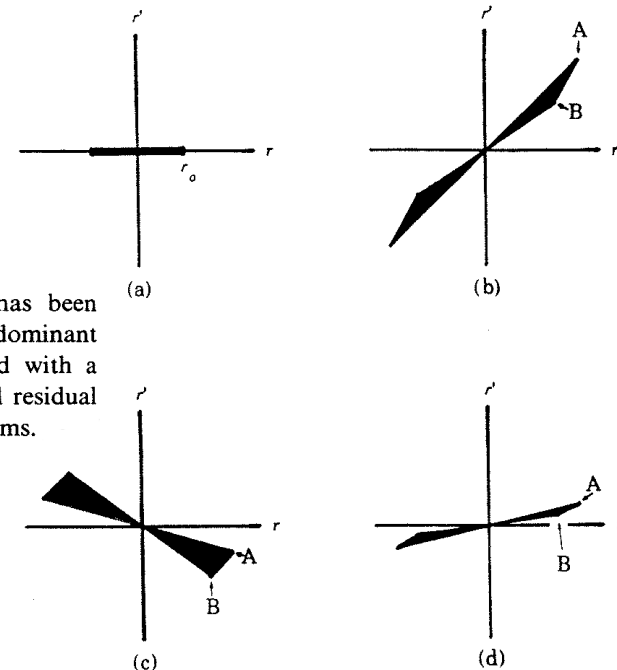


Fig. 3. Transverse phase-space plots showing emittance growth and reduction. (a) Initial phase-space plot with very small emittance. (b) Phase space plot after drift z_1 to lens, showing the emittance growth due to the different expansion rates of points A and B. (c) Phase-space plot immediately after lens, showing rotation due to the lens. The emittance is unchanged because we assume the lens is linear. (d) Phase space plot after drift z behind lens, showing the emittance reduction due to the different expansion rates of points A and B.

Emittance compensation from envelope eqn.

Serafini and Rosenzweig used envelope equation to explain emittance compensation (Phys. Rev. E **55** (1997) 7565).

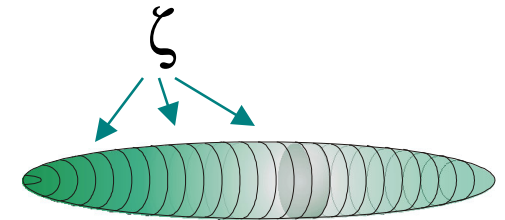
$$\sigma'' + \sigma' \frac{\gamma'}{\beta^2 \gamma} + \sigma K_r - \frac{I(\zeta)}{\sigma 2I_0 \beta^3 \gamma^3} - \frac{\epsilon_n^2}{\sigma^3 \beta^2 \gamma^2} = 0$$

includes solenoid and RF ζ tags long. slice in the bunch

For space charge dominated case in absence of acceleration

$$\cancel{\sigma'' + \sigma' \frac{\gamma'}{\beta^2 \gamma} + \sigma K_r} - \frac{I(\zeta)}{2\sigma I_0 \beta^3 \gamma^3} - \cancel{\frac{\epsilon_n^2}{\sigma^3 \beta^2 \gamma^2}} = 0$$

Brillouin flow $\sigma'' \rightarrow 0$: $\sigma_{eq} = \sqrt{\frac{I(\zeta)}{2K_r I_0 \beta^3 \gamma^3}}$



Emittance compensation (contd.)

Oscillations near equilibrium: $\delta\sigma'' + \delta\sigma \left[2K_r - \frac{\delta\sigma}{\sigma_{eq}} + \left(\frac{\delta\sigma}{\sigma_{eq}} \right)^2 - \dots \right] = 0$

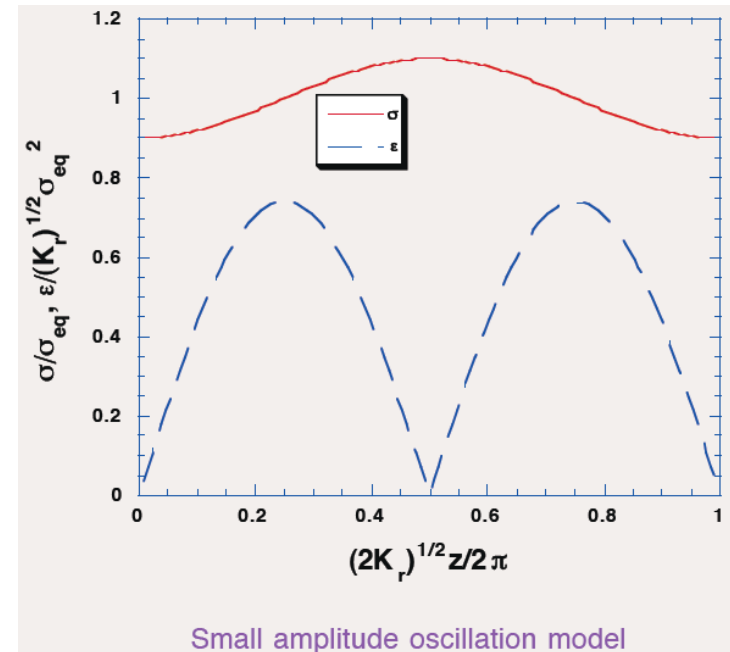
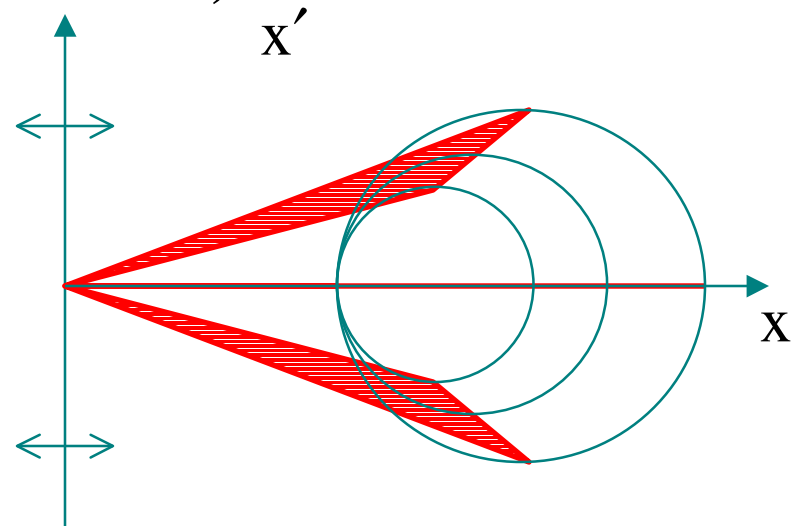
Important: frequency of small oscillations around equilibrium does not depend on ζ . E.g. for beam with $\sigma'(0, \zeta) = 0$ and $\sigma(0, \zeta) = \sigma_{eq}(\zeta) + \delta\sigma(\zeta) = \sigma_0$:

$$\begin{cases} \sigma(z, \zeta) = \sigma_{eq}(\zeta) + \delta\sigma(\zeta) \cos(\sqrt{2K_r} z) \\ \sigma'(z, \zeta) = -\sqrt{2K_r} \delta\sigma(\zeta) \sin(\sqrt{2K_r} z) \end{cases}$$

$$\varepsilon = \frac{1}{2} \sqrt{\langle r^2 \rangle \langle r'^2 \rangle - \langle r'r \rangle^2} \approx \sqrt{2K_r} \langle \sigma_{eq} \rangle \sigma_0 \left| \sin(\sqrt{2K_r} z) \right|$$

Emittance compensation (contd.)

- slices oscillate in phase space around different equilibria but with the same frequency
- ‘projected’ emittance reversible oscillations when $\delta\sigma/\sigma_{eq} \ll 1$, unharmonicity shows up when $\delta\sigma$ is not small
- ignores the fact that beam aspect ratio can be $\gg 1$ (e.g. at the cathode)



Emittance compensation (contd.)

Including acceleration term and transforming from $(\sigma, z) \rightarrow (\tau, y)$ in the limit $\gamma \gg 1$

$$\frac{d^2\tau}{dy^2} + \Omega^2\tau = \frac{e^{-y}}{\tau}$$

$y \equiv \ln \frac{\gamma}{\gamma_0}$, $\tau \equiv \sigma \gamma' \sqrt{\gamma_0 / (I(\zeta) / 2I_0)}$, Ω represents solenoid & RF focusing

Particular solution that represents generalized Brillouin flow or ‘invariant envelope’:

$$\tau_{eq} = \frac{2e^{-y/2}}{\sqrt{1+4\Omega^2}}, \quad \sigma_{eq} = \frac{2}{\gamma'} \sqrt{\frac{I(\zeta)}{\gamma 2I_0} \frac{1}{1+4\Omega^2}}$$

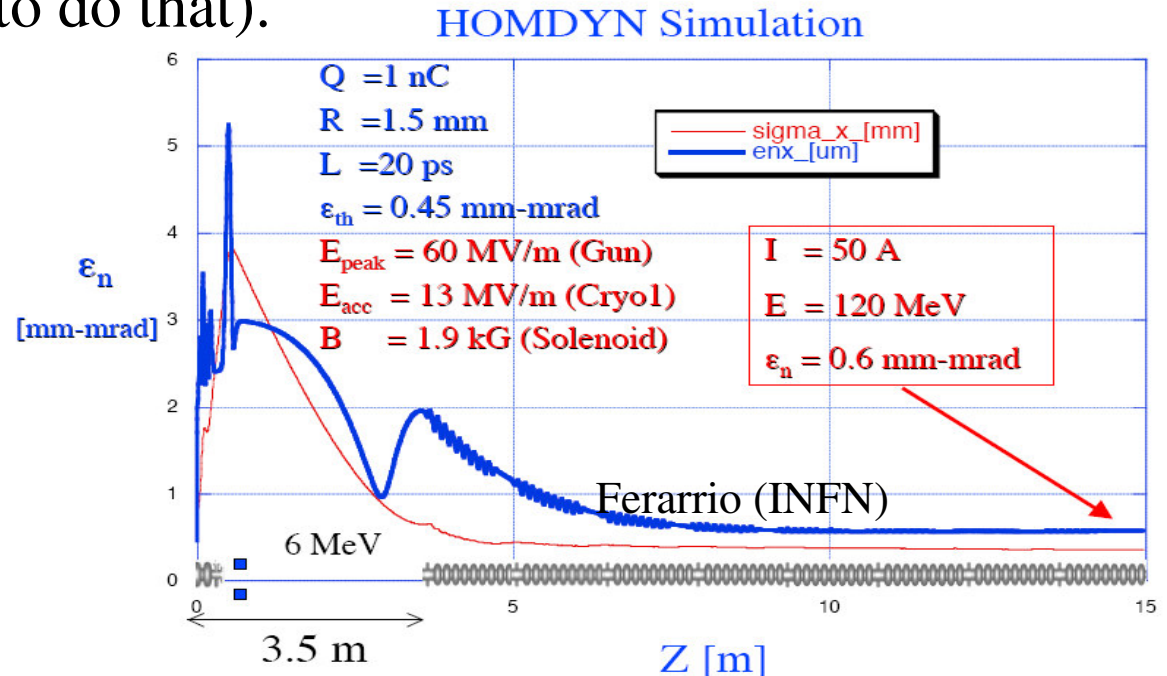
$\frac{\gamma\sigma'_{eq}}{\sigma_{eq}} = -\frac{\gamma'}{2}$ phase space angle is independent of slice ζ

Matching beam to ‘invariant envelope’ can lead to ‘damping’ of projected rms emittance.

Emittance compensation and tracking

Serafini and Rosenzweig's paper provides a recipe for emittance compensation, which works for simple cases (e.g. matching beam into long focusing channel / linac in the injector). For other more complicated scenarios one can try solving envelope equation for slices (or write a code to do that).

Particle tracking is indispensable for analysis and design of the injector where the assumptions made are invalid or theory is too complicated to be useful.



Computer Modeling

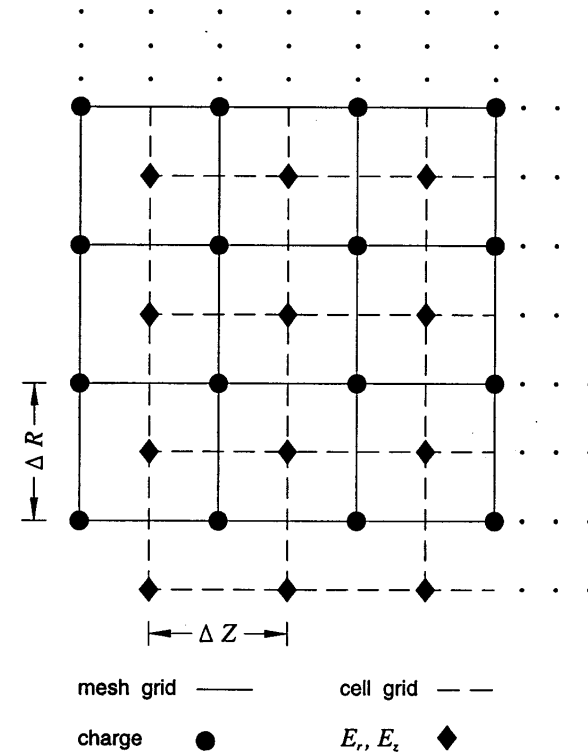
- It used to be the case that extensive modeling of the injector was too demanding in terms of time & computer resources to allow finding optima for generating bright beams by varying more than a couple (or so) parameters.
- This is no longer true. Advances in space charge codes & computing abilities allow extensive study / optimization of nonlinear space charge problem in the injector with good precision and minimal number of assumptions.
- Numerical studies can give insights and better understanding of beam dynamics in the injector.

Space charge codes

Different approaches are used (e.g. envelope equation integration, macroparticle tracking, various meshing scenarios, etc.).

Mesh method works as following:

- 1) transform to rest frame of the reference particle
- 2) create mesh (charge) and cell grid (electrostatic fields)
- 3) create table containing values of electrostatic field at any cell due to a unit charge at any mesh vertex (does not need to be recalculated each time step)



Space charge codes (contd.)

4) assign macroparticle charges to mesh nodes, e.g. 1,2,3, and 4 vertices get QA_1/A , QA_2/A , QA_3/A , and QA_4/A respectively, where $A_1+A_2+A_3+A_4 = A = \Delta Z \Delta R$

5) calculate field at each cell by using mesh charges and table, e.g.

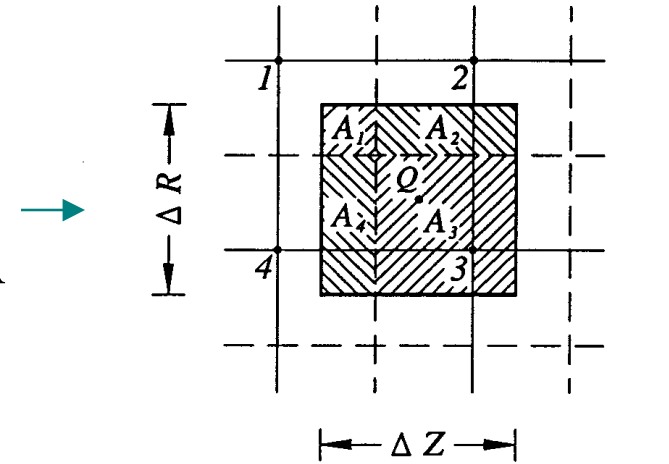
$$\vec{E}(1), \vec{E}(2), \vec{E}(3), \vec{E}(4)$$

6) find fields at macroparticle position by weighting

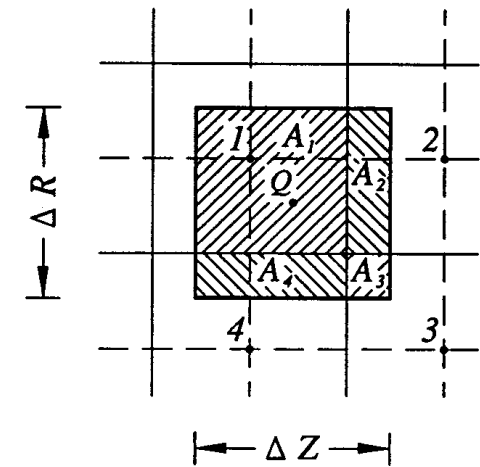
$$(A_1 \vec{E}(1) + A_2 \vec{E}(2) + A_3 \vec{E}(3) + A_4 \vec{E}(4)) / A$$

7) Apply force to each macroparticle

8) Lorentz back-transform to the lab frame

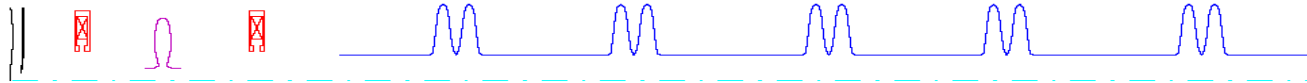


mesh grid ——— cell grid - - -



mesh grid ——— cell grid - - -

Example of injector optimization



Fields:

DC Gun Voltage (300-900 kV)
2 Solenoids
Buncher
SRF Cavities Gradient (5-13 MV/m)
SRF Cavities Phase

Positions:

2 Solenoids
Buncher
Cryomodule

Bunch & Photocathode:

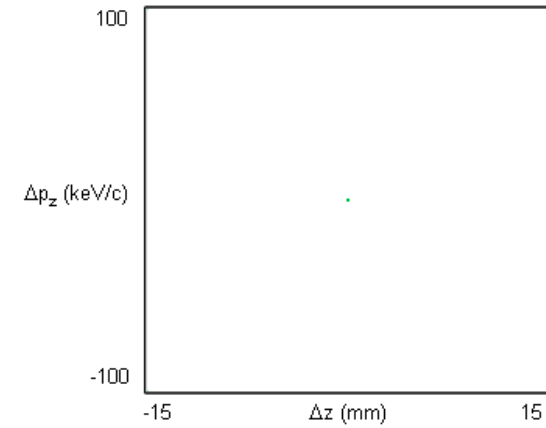
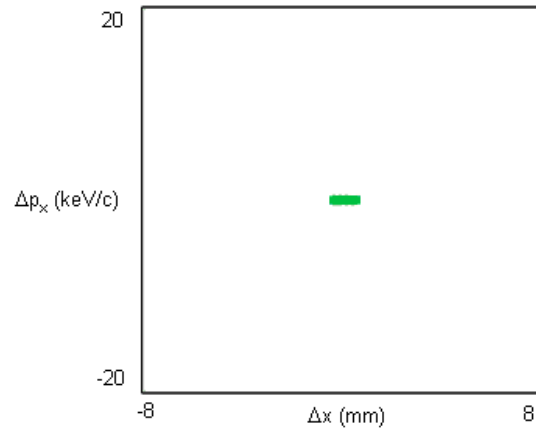
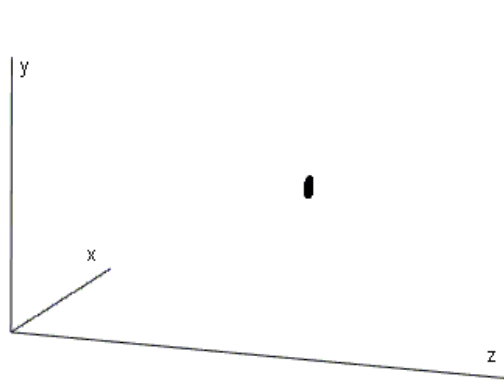
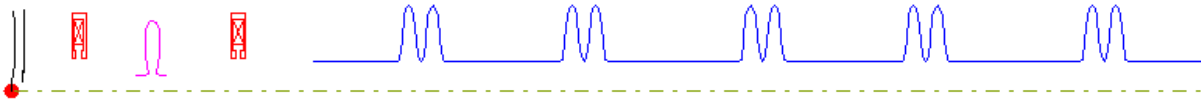
E_{thermal}
Charge

Laser Distribution:

Spot size
Pulse duration (10-30 ps rms)
{tail, dip, ellipticity} x 2

Total: 22-24 dimensional parameter space to explore

Examples of beam dynamics: 80 pC charge



$z = 0.000$ m

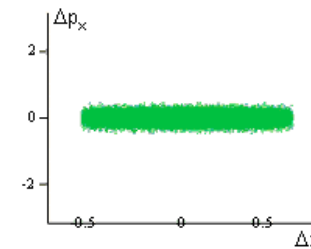
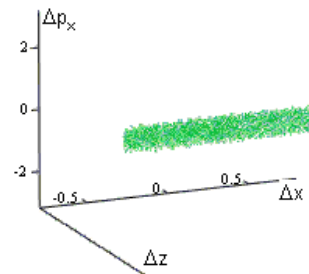
$p_z = 0.000$ MeV/c

$\sigma_x = 0.294$ mm

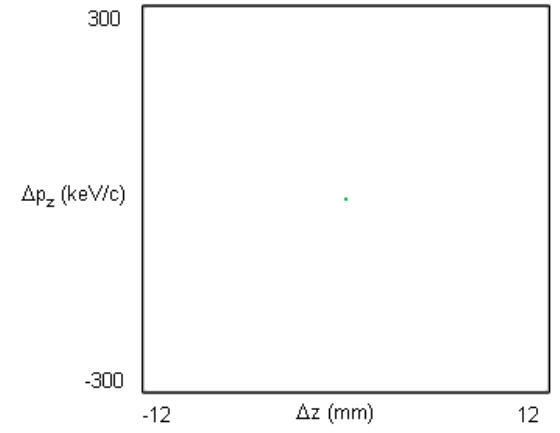
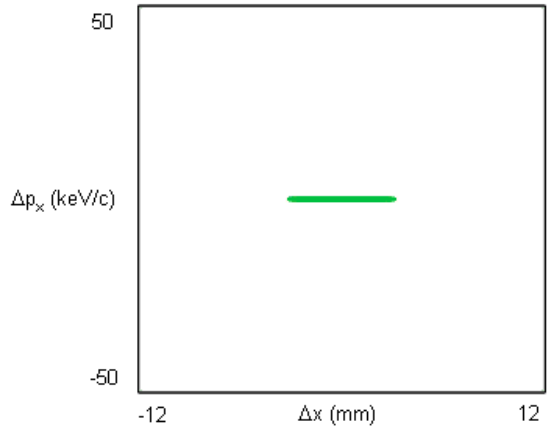
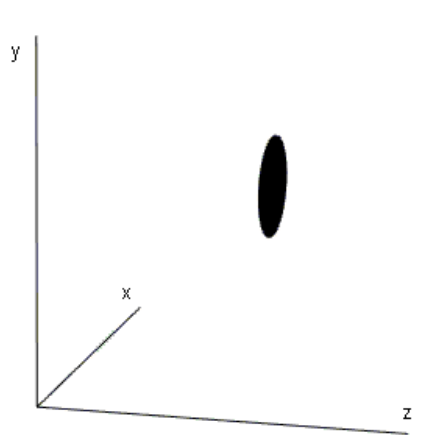
$\epsilon_x = 0.077$ mm-mrad

$\sigma_z = 0.000$ mm

$\epsilon_z = 0.000$ mm-keV



Examples of beam dynamics: 0.8 nC charge



$z = 0.000$ m

$p_z = 0.000$ MeV/c

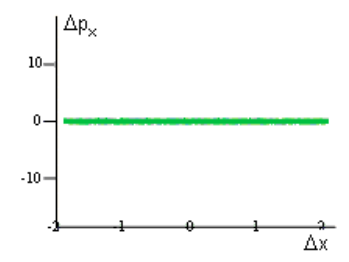
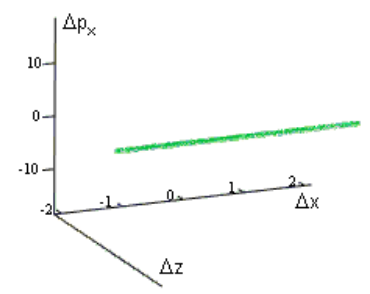
$\sigma_x = 1.629$ mm

$\epsilon_x = 0.425$ mm-mrad

$\sigma_z = 0.000$ mm

$\epsilon_z = 0.000$ mm-keV

Zoomed in transverse phase space



Injector performance

Takes several 10^5 simulations

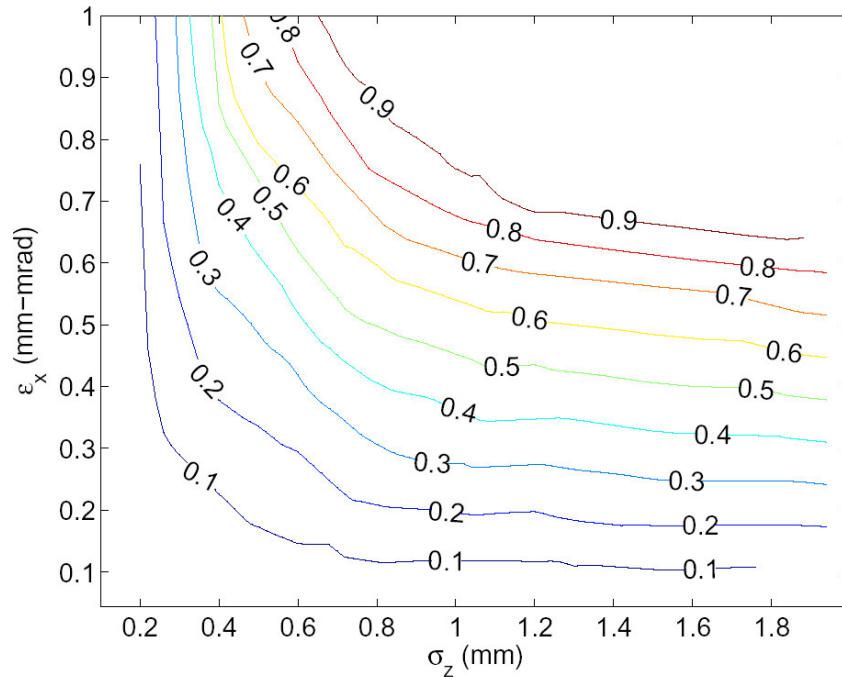


FIG. 10: Transverse emittance vs. bunch length for various charges in the injector (nC).

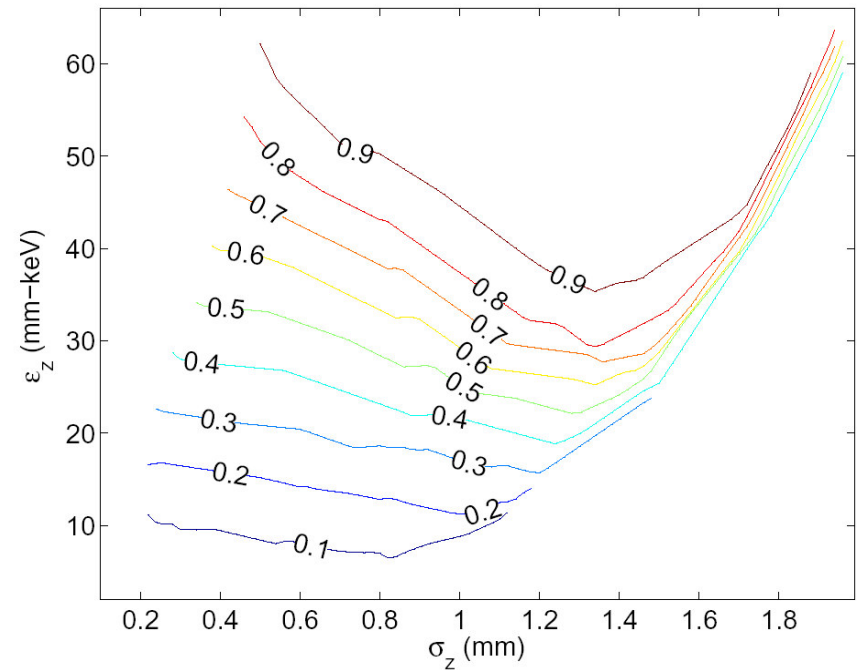


FIG. 11: Longitudinal emittance vs. bunch length for various charges in the injector (nC).

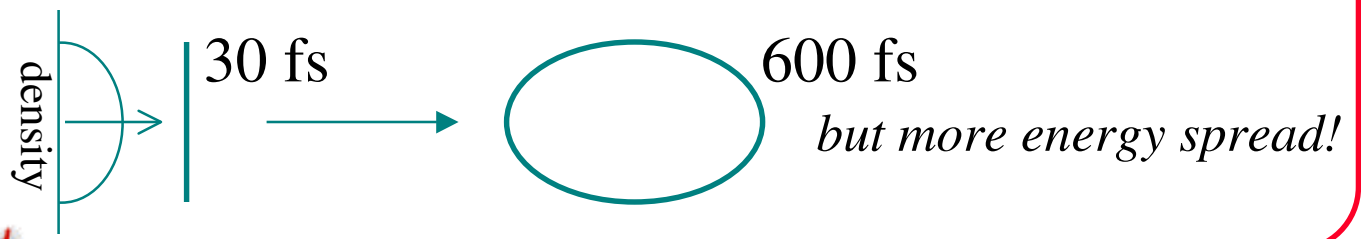
$$\epsilon_n [\text{mm-mrad}] \approx (0.73 + 0.15/\sigma_z [\text{mm}]^{2.3}) \times q [\text{nC}]$$

Optimal initial (laser) distribution

If space charge force is linear within a bunch, there is no rms emittance growth associated with it. Uniform transverse distribution for cylindrical continuous beam is one example. For bunched beam, 3D ellipsoid satisfies the requirement

$$\frac{x^2}{A^2} + \frac{y^2}{B^2} + \frac{z^2}{C^2} = 1, \quad \vec{E} = (E_x, E_y, E_z) = \frac{3q}{4\pi\epsilon_0 ABC} (M_x x, M_y y, M_z z)$$

Under linear self-forces, the shape will remain to be elliptical. Luiten et. al suggested using elliptical 2D shape ‘ δ -function’ laser pulse (~ 30 fs) to produce 3D ellipsoid under the influence of space charge near the cathode (PRL **93** (2004) 094802).



Optimal initial (laser) distribution (contd.)

Several things change the idealistic 3D ellipsoid picture:

- 1) image charge at the cathode
- 2) distortion due to bunching

*example for DC gun
optimal shape (80 pC)*

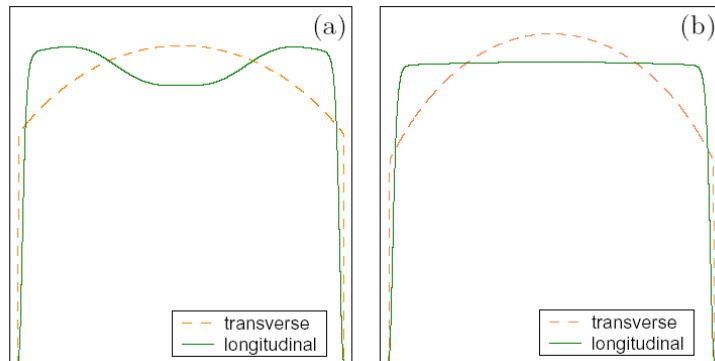


FIG. 6: Initial distribution profiles corresponding to minimal emittance at the end of the injector for (a) 80 pC and (b) 0.8 nC cases.

Phys. Rev. ST-AB **8** (2005) 034202

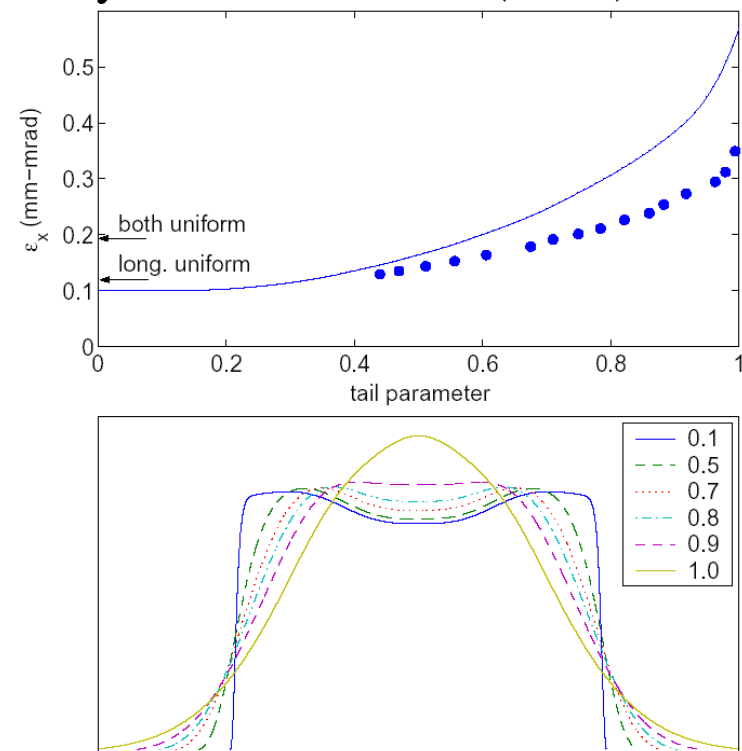
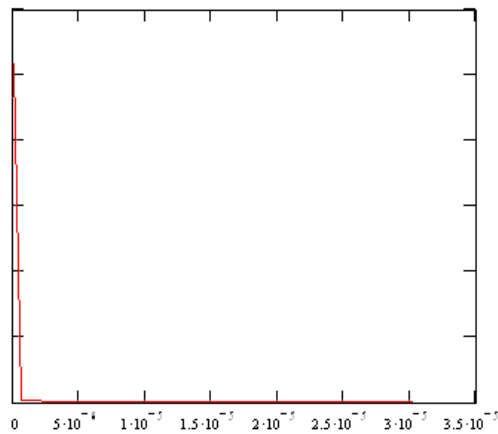
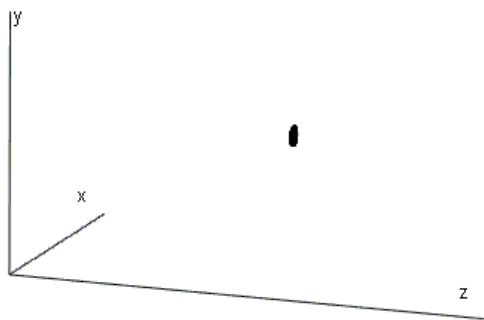
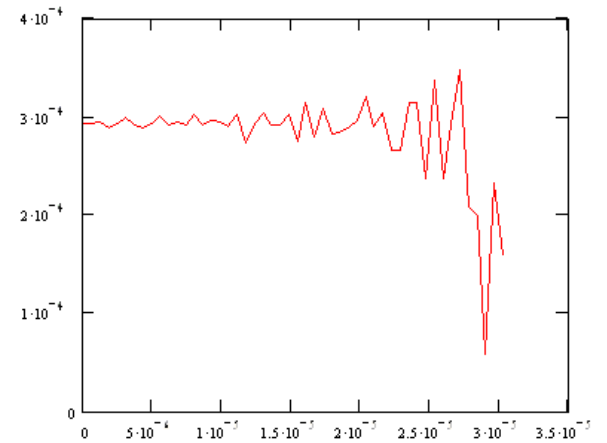


FIG. 7: 80 pC: emittance sensitivity (solid curve) to the longitudinal profile changes (top) and the corresponding profile shapes (bottom).

Example of profile evolution: 80 pC charge



Longitudinal Profile (abscissa slice position in m)



(y-axis) Slice Rms size (m) vs. (x-axis) slice coordinate (m)

$z = 0.000$	m	$\epsilon_x = 0.077$	mm-mrad	$\sigma_x = 0.294$	mm
$p_z = 0.000$	MeV/c	$\epsilon_z = 0.002$	mm-keV	$\sigma_z = 0.003$	mm

Technology: some highlights

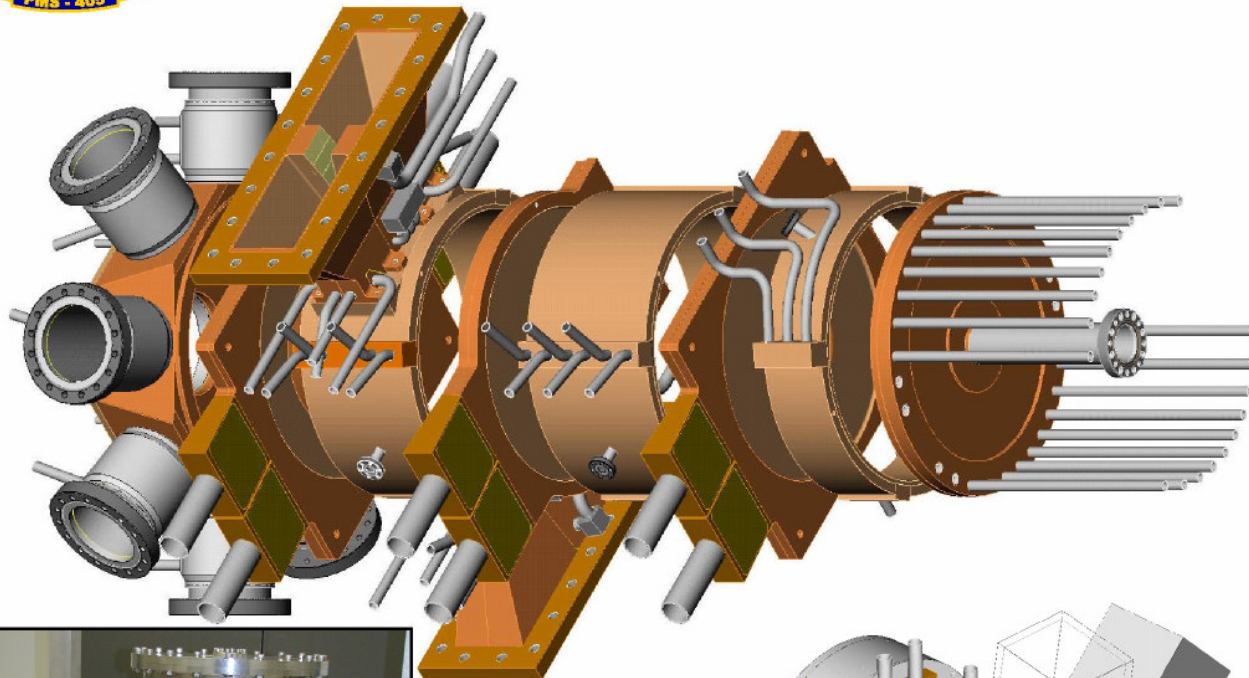
	DC Gun	Normal RF	SRF Gun
Max Gradient (achieved)	4.3 MV/m	6 MV/m	32 MV/m
Max Gradient (planned)	> 7 MV/m	10 MV/m	> 20 MV/m
Max current (demonstrated)	10 mA	128 mA at 25% DF	1 mA
Max current (planned)	100 mA	1000 mA	500 mA
Issues	Field emission Vacuum Ion back bombardment	Thermal Management Vacuum	Thermal management Contamination of SRF cavity

NCRF gun

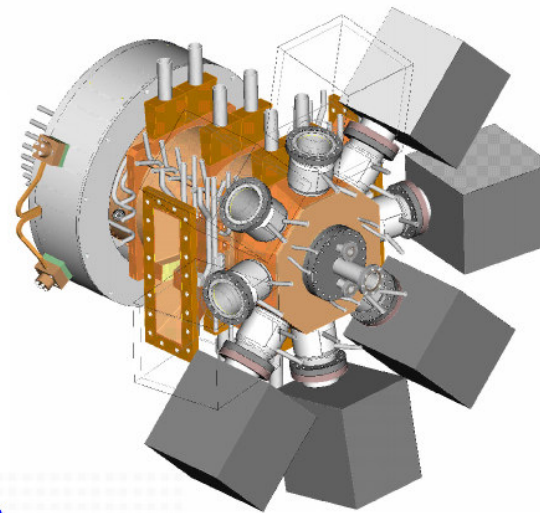
- Arguably the best gun choice for low duty beam – so far the brightest injector beam (low duty factor) was measured from a NCRF gun
- Boeing FEL project has demonstrated high average current capability (still the highest ave. current)
- Ohmic wall losses pose heat management challenge → gradient < 10 MV/m for CW operation
- As a result, maintaining good vacuum condition is difficult, which affects cathode lifetime
- LANL/AES project seeks to produce 1 A beam from a NCRF gun



RF Photoinjector Summary (Dowell)



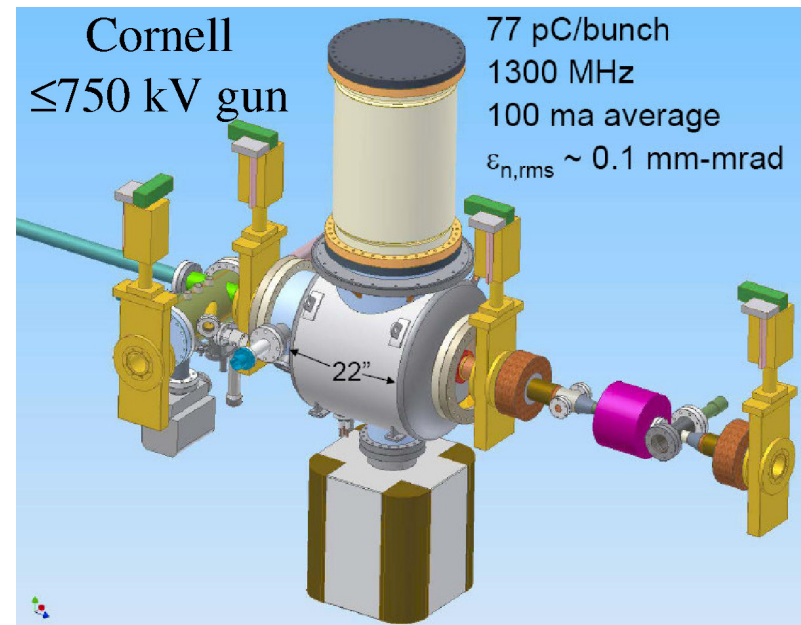
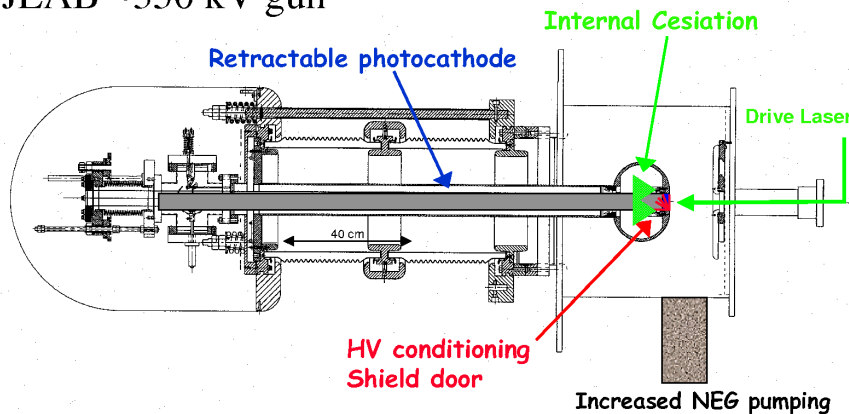
Gun Type	RF
Injector and ERL	
RF Frequency (MHz)	700
PRF (MHz)	33.3 (350)
Charge/Bunch (nC)	3.0
Current (mA)	100 (1050)
Injector Energy (MeV)	2.5
Transverse RMS Normalized Emittance	6
Longitudinal RMS Emittance (keV-psec)	145
RMS Bunch Length (psec)	
RMS Energy Spread (%)	0.5
ERLP Energy (MeV)	N/A
ERL Energy Goal (MeV)	N/A
Electron Gun	
DC Gun Voltage (kV)	N/A
Gun Accelerating Field (MV/m)	7 / 7 / 5
Cathode Material	Multi-Alkali
Drive Laser FWHM Pulse Length (psec)	16
Laser Wavelength (nm)	527
Laser Power at 5% QE (W)	5 (53)
Booster Accelerator	
Type	N/A
Geometry (Cavities x Cells)	1 x 2.5
Couplers per Cavity / Type	2 / WG
Coupler Power (kW)	500
Status	Fabrication



DC gun

- 3 ongoing ERL projects are planning / using this type
- Operation at higher fields (~ 10 MV/m) than demonstrated is crucial for good emittance \rightarrow field emission gradient \rightarrow polishing / dielectric coating
- Cathode lifetime is an issue for all high average current ERLs \rightarrow ion backbombardment and cathode chemical poisoning \rightarrow exceptional vacuum

JLAB ~ 350 kV gun



SRF gun

- Avoids wall losses problem of NCRF guns
- Higher peak field than in DC gun (~ 50 MV/m)
- Cathode issues: contamination & thermal management
- Superconductor does not allow putting magnetic field close to the cathode. Possible solutions:
 - wall retraction
 - magnetic mode
 - downstream focusing

Rossendorf 1.3 GHz 3.5 Cell SRF Gun

Cavity: Niobium 3+1/2 cell
(TESLA Geometry)
Choke filter

Operation: T = 1.8 K

Frequency: 1.3 GHz

HF power: 10 kW

Electron energy: 10 MeV

Average current: 1 mA

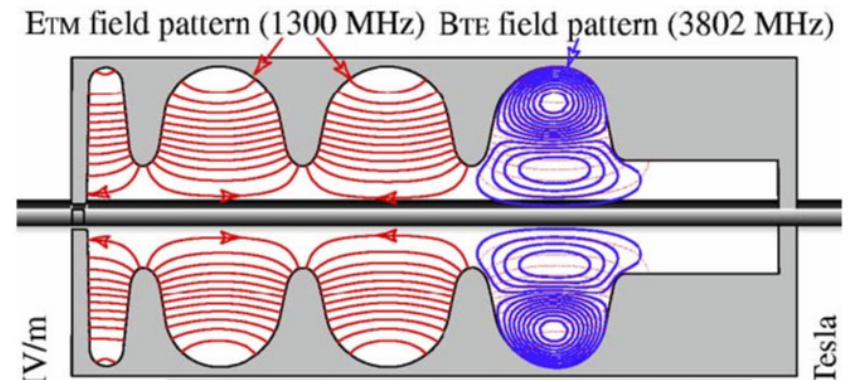
Cathode: Cs₂Te
thermally insulated, LN₂
cooled

Laser: 262 nm, 1W

Pulse frequency: 13 MHz & < 1 MHz

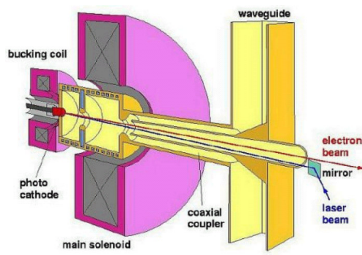
Bunch charge: 77 pC & 1 nC

Janssen



DC/SFR/NCRF: emit. compensation works

NCRF



pulsed!

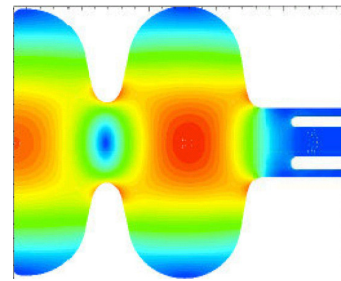
$$E_{\text{cath}} = 120 \text{ MV/m}$$

$$\tau_{\text{laser}} = 2.7 \text{ ps rms}$$

$$\sigma_{\text{laser}} = 0.5 \text{ mm rms}$$

$$\tau_{\text{laser}} \rightarrow z = 0.08 \text{ mm}$$

SRF



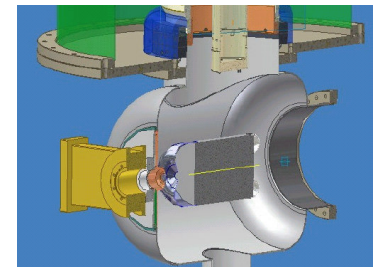
$$E_{\text{cath}} = 43 \text{ MV/m}$$

$$\tau_{\text{laser}} = 5.8 \text{ ps rms}$$

$$\sigma_{\text{laser}} = 0.85 \text{ mm rms}$$

$$\tau_{\text{laser}} \rightarrow z = 0.12 \text{ mm}$$

DC

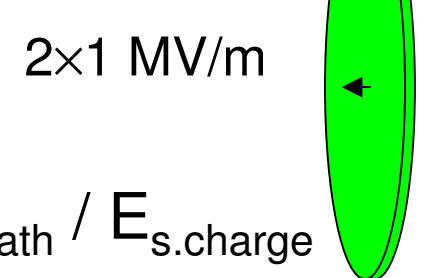
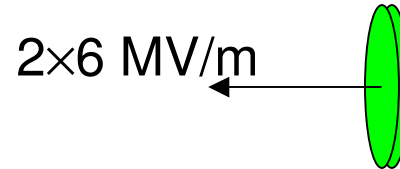


$$E_{\text{cath}} = 8 \text{ MV/m}$$

$$\tau_{\text{laser}} = 13 \text{ ps rms}$$

$$\sigma_{\text{laser}} = 2 \text{ mm rms}$$

$$\tau_{\text{laser}} \rightarrow z = 0.12 \text{ mm}$$



$$E_{\text{cath}} / E_{\text{s.charge}} = E_{\text{cath}} / E_{\text{s.charge}} = E_{\text{cath}} / E_{\text{s.charge}}$$

Thermal emittance and cathode field!

Emittance compensation can be achieved despite reduced flexibility in solenoid positioning

	Q [nC]	Rms bunch Length (compressed)	Ex [mm-mrad]	Cathode material(&)	Band Peak field
RF	1 / 0.2	2.8 ps / 1.7 ps	0.72 / 0.3 (**)	Copper, 700 meV	S-Band [120 MV/m]
DC	1/ 0.1	3ps / 3ps	0.8 / 0.14 (**)	GaAs 35 meV	[15 MV/m] (Average)
SRF	1 / 0.1(*)	5.7 ps/ 2.7 ps	0.8 / 0.23 (**)	"metallic" 184 meV	L-Band [60MV/m]

(*) scaled

(**) limited by thermal emittance

(&) Copper and GaAs use measured values, but SRF gun uses generic metallic cathode number for thermal emittance (0.3 mm-mrad per 1 mm full radius)

$$\varepsilon_n [\text{mm - mrad}] \geq 4 \sqrt{\frac{q[\text{nC}]E_{th}[\text{eV}]}{E_{cath}[\text{MV/m}]}}$$

RF and DC guns computations are based on optimum emission pulse "3D-ellipsoid", whereas SRF gun computation uses "beer can"

Photocathode requirements & technology

- Ideal photocathode has little thermal emittance, high QE, fast response time, and robust (lifetime!)
- NEA GaAs photocathodes seem to fit DC guns nicely (longish pulse OK due to downstream compression, good thermal emittance allows lower operating field), may be too long for RF guns for lowest emittance
- Optimal wavelength for GaAs may be not near the band-gap, e.g. shorter wavelength → faster response time → better temporal shape vs. poorer thermal emittance trade-off
- Multialkali cathodes demonstrate good lifetime, QE, and fast response, somewhat inferior thermal emittance, need higher photon energy
Semiconductor superlattice theoretically allows superior performance to bulk semiconductors both in terms of QE, smaller thermal emittance

Cathodes for ERLs

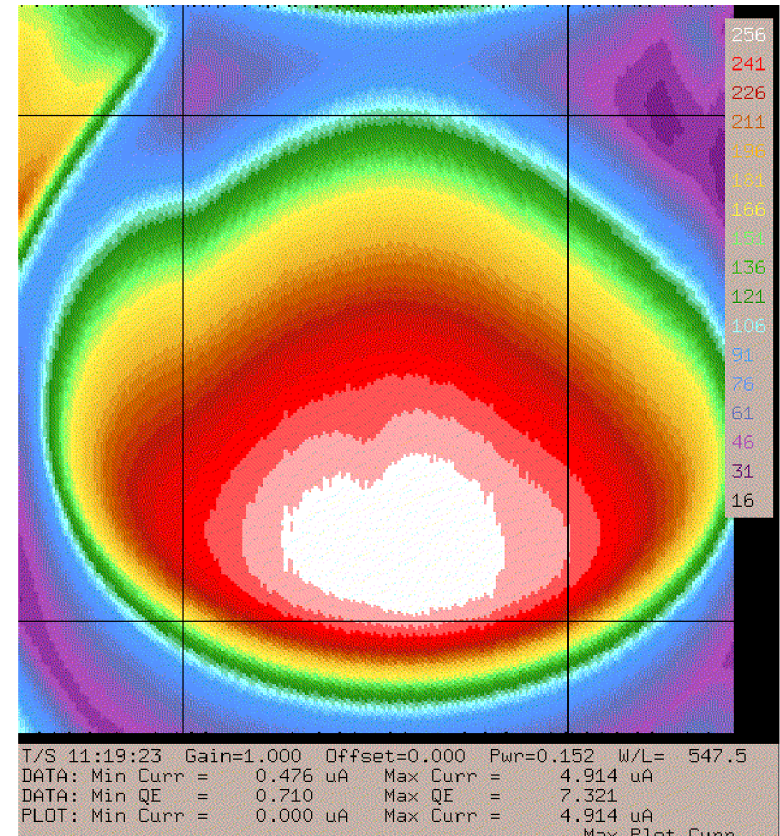
- 100 mA +
 - Cs:GaAs (demonstrated 9 mA CW, DC JLab FEL)
 - K_2CsSb (demonstrated 128 mA at 25% d.f., NCRF Boeing)
 - Cs_3Sb
- 10 mA +
 - Cs: GaAs (polarized), and Cs_2Te
- 1 mA +
 - Metals, Dispenser cathodes
- Technologies to watch (not demonstrated in injectors yet)
 - Cs dispenser cathode, Cs:GaAsP, Cs:GaN, and Diamond

GaAs photocathode performance (Hernandez-Garcia): **over 450 C delivered without QE replenishing!**

- 3 months without re-cesiation
- About 96% of previous QE is recovered with each re-cesiation
- Established 5.23% QE by measuring drive laser power at 55 mW to get 1.1 mA CW at 135pC, while the scanner reported 2% QE
- For new cathode, scanner reports ~7% QE, then the extrapolated initial QE should be ~15%

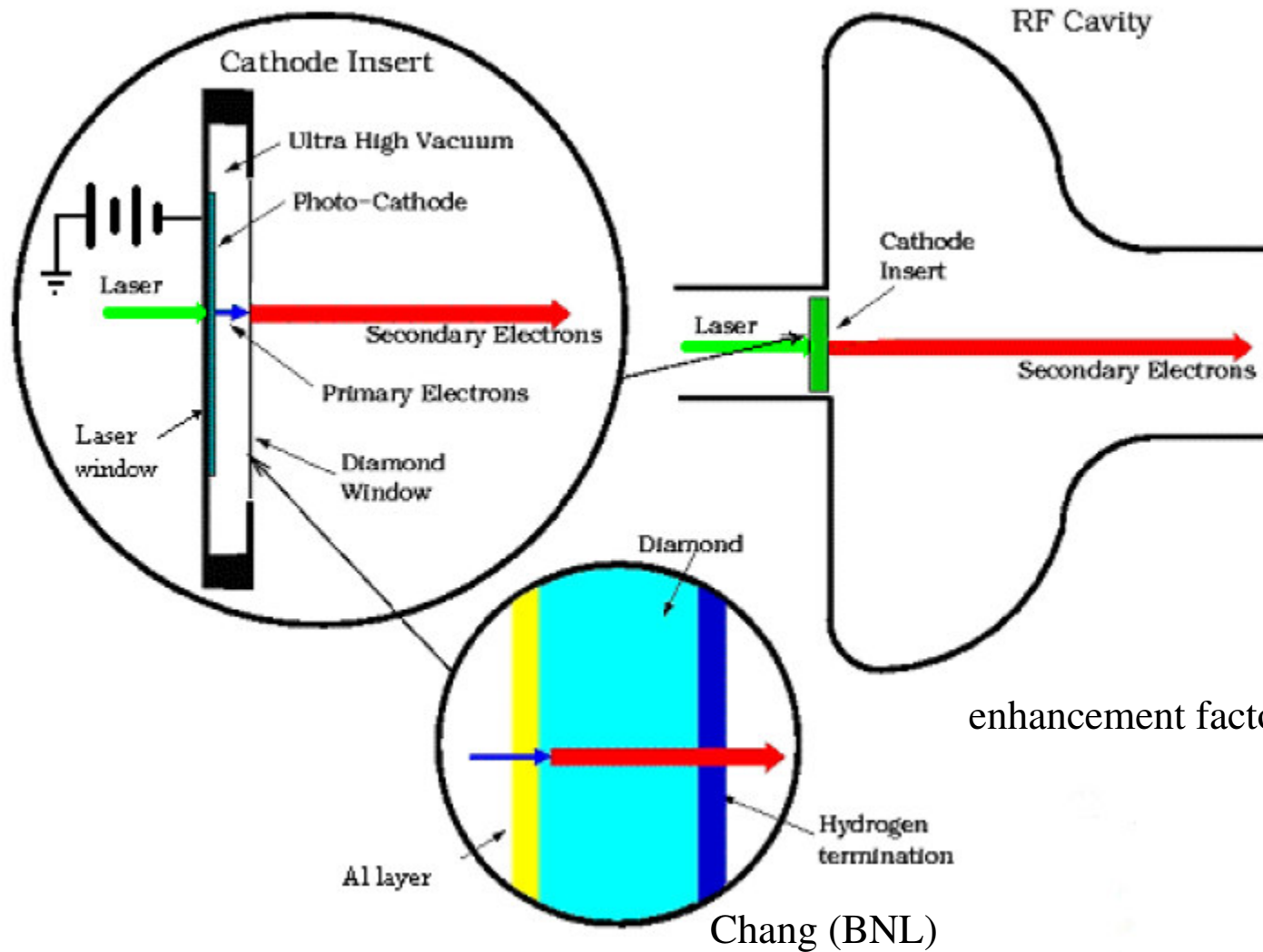
	Beam time (hours)	Delivered charge (Coulombs)
Pulse	131:03	56
CW	43:55	417-450
Overall totals	174:58	473-506

Cathode Archiver by W. Moore and A. Grippo



Typical cathode scan using green He-Ne

Diamond secondary emission cathode idea

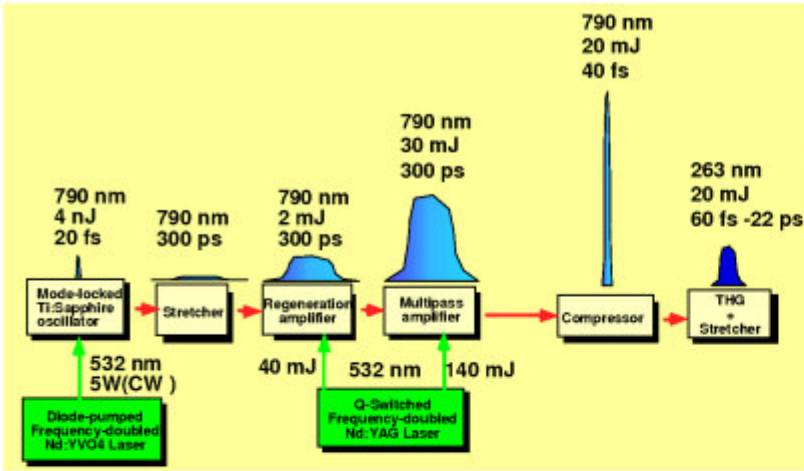


Laser

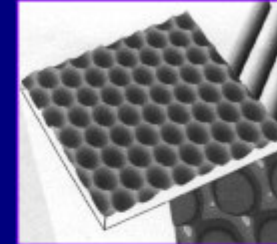
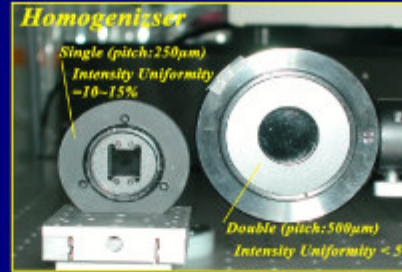
- Critical component of each photoinjector, any laser problems propagate along the entire accelerator
- R&D challenges in meeting shape requirements for best beam dynamics, programmable time structure of pulses
- For light sources with pump-probe experiments, timing synchronization between electron pulses and pump laser requires ~ 10 fs synchronization (\sim km distributed timing system)

Parameter	Electron cooling ERL	High Current ERL	Polarized e-Source ERL
Current (mA)	500	100	24
PRF (MHz)	28	700	15
Wavelength (nm)	530	530	780
QE(%)	2	2	0.3
Laser System	Yb Fiber MOPA w/SHG	Yb Fiber MOPA w/SHG	Er Fiber MOPA w/SHG
Cathode Power (W)	70	15	30

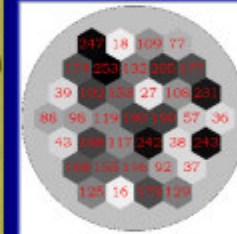
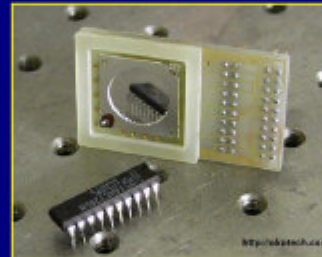
Temporal & transverse pulse shaping



Spatial profile shaping with **MicroLens Array**

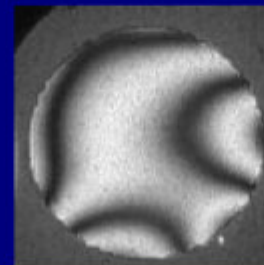
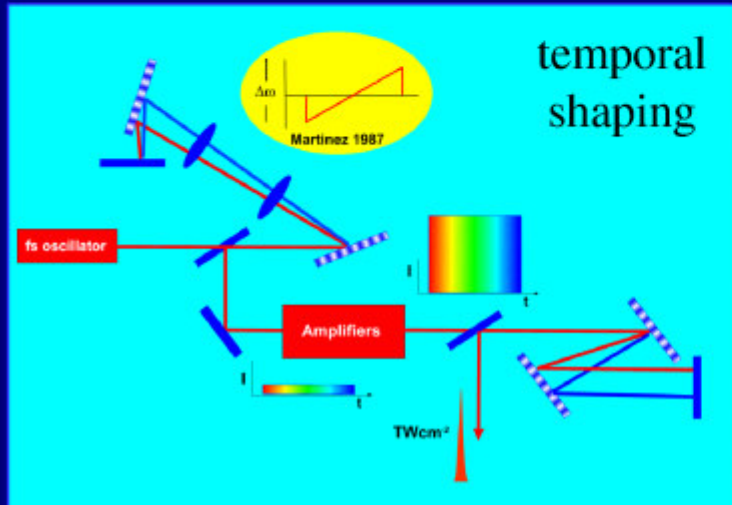


Spatial profile shaping with **Deformable Mirror**



Genetic Algorithms

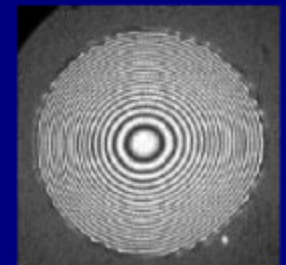
control loop dynamically adjusts shape



Initial State
(All: 0V)



Random Voltage



All: 125V

Problems

- 1) In computer simulations of the space charge inside the bunch, one uses ‘macroparticles’ with the same charge to mass ratio to reduce the required computational resources. Discuss what happens to simulated beam’s Debye length and plasma frequency as opposed to real case scenario. In this respect, what artificial effects may be introduced in simulations?
- 2) Show that transformation of phase ellipse parameters for a drift $0 \rightarrow z$ are given by

$$\begin{aligned} B &\rightarrow B - 2Az + \Gamma z^2 \\ A &\rightarrow A - \Gamma z \\ \Gamma &\rightarrow \Gamma = \text{const} \end{aligned}$$

Books

M. Reiser, Theory and design of charged particle beams, Wiley & Sons, 1996

J.D. Lawson, The physics of charged-particle beams, Oxford Press, 1988

Also free online books at <http://www.fieldp.com/educa.html>

M. Rabinovitz, “Electrical conductivity in high vacuum”, SLAC-TN-68-23

J.I. Pankove, Optical processes in semiconductors, Prentice-Hall, 1971